XA0055583

Experiments on the Behaviour of Thermite Melt Injected into Sodium - Final Report on the THINA Tests Results

F. Huber, A. Kaiser, W. Peppler
Kernforschungszentrum Karlsruhe
Institut für Reaktorsicherheit
Postfach 3640
76021 Karlsruhe, Germany

Abstract

During hypothetical accidents of fast breeder reactors the core melts and part of the core material inventory is ejected into the upper coolant plenum. As a consequence, a fuel to coolant thermal interaction occurs between the melt and the sodium. A series of simulating experiments was carried out in KfK/IRS to improve the knowledge about the phenomenology of molten fuel/coolant interactions and to support theoretical work on the safety of fast breeder reactors. In the tests, a thermite melt of up to 3270 K is injected from below into a sodium pool the temperature of which is between 770 and 820 K. The masses of the melt and the sodium are about five and 150 kg, respectively. Thermal interactions have been observed to occur as a sequence of small local pressure events mainly during the melt injection. Large-scale vapour explosions have not been observed. Generally, the conversion ratios of thermal to mechanical energy have been low.

1. INTRODUCTION

The analysis of core disruptive accidents with an extremely low probability of occurrence in liquid-metal cooled fast breeder reactors (LMFBRs) shows that the core may undergo melting. Mass relocation and freezing may lead to the formation of a pool in a bottled-up configuration containing molten core materials [1]. It is further assumed that the enclosure of the liquid pool ultimately loses its integrity and a multi-phase mixture of molten fuel and steel is discharged from the core into the upper and/or lower coolant plenum which leads to fuel coolant thermal interactions.

To improve knowledge in this field, a series of out-of-pile experiments was carried out at KfK in the so-called THINA test facility. There, the molten core material was simulated by a thermite melt composed of alumina and iron. The melt was injected from below into a sodium-filled vessel, which simulated the upper coolant plenum. The main objective of these experiments was to investigate the phenomenology and physics of thermal and hydraulic interactions of the melt and the sodium. Information was derived on penetration depths of the melt, the development of the two-phase region, the ratio of conversion of thermal into mechanical energy, and fragmentation of the melt. Special interest was devoted to the question of highly energetic thermal interactions. The experimental data were also used to validate the multiphase fluid dynamics computer code AFDM [2]. Preliminary results of the tests have been published previously [3, 4].

In this paper a survey is given of four tests performed with the so-called compact injector. The main experimental issues are discussed such as spatial void development, characteristics of the interaction of melt and sodium, and energy conversion ratio.

2. TEST FACILITY

The two major parts of the test set-up are the test vessel to simulate the sodium plenum and the injector system to generate the melt and to inject it. Both are described in the following; further information can be found in Refs. 3 and 4.

2.1 Test Vessel and Instrumentation

The test vessel and the instrumentation are shown in Fig. 1. The vessel has a diameter of 0.3 m and a height of 5 m. About one half of the vessel is filled with sodium above which a cover gas space serves as an expansion volume. The small diameter was chosen to facilitate application of the X-ray technique. At a height

of 2 m above the bottom, a perforated plate is mounted which reduces the open cross section to 33 %. The plate acts as additional flow resistance for the sodium column during both the expansion and collapse of the two-phase region. As a result, the sodium moves slower in both directions, and the dynamic stresses of the vessel during the final collapse "water hammer" are reduced. Because of the geometry chosen the results cannot be transfered directly to reactor conditions.

To be able to observe the course of events during the thermal interaction, the vessel is instrumented with five pressure transducers to measure pressures in the sodium and in the cover gas, with more than one hundred temperature and void sensors installed on horizontal lances, four sensors on each lance, with a level indicator, and with four X-ray facilities supplying both high speed movies and analog signals from an array of photo diodes. The diode signals are calibrated to give the mean cross-sectional void fraction. From the temperature and void sensors and from the diode signals, information is derived on the temporary and spatial development of the two-phase region. These measurements are essential for understanding the physical processes and provide a data base for model and code validation.

The disadvantage of temperatur and void sensors is that, if contacted by the melt, they are normally destroyed prior to the end of the experiment. The X-ray facilities positioned at various heights allow to observe the melt injection and the development of the two-phase region during the whole test.

Pressure transducers P61, P62, and P63 whose axial positions are indicated in Fig. 1 register the pressure in the sodium near the vessel wall. Pressure transducers P64 and P003 register the pressures in the gas space above the sodium and in the gas supply pipe, respectively.

The level indicator mounted vertically at a distance of 30 mm from the vessel wall measures the local changes in the sodium level.

2.2 Melt Injector System

A gas driven injection system is used that is able to inject about 5 kg of melt. The melt consisting of alumina and iron is generated in a crucible by an exothermal reaction of an aluminium/iron oxide thermite mixture. The reaction products separate during and after the reaction because of their different densities. The use of modified crucibles allows to inject mainly alumina or mainly iron (Fig. 2).

The temperature of the melt depends on the intial temperature of the thermite mixture, on the heat losses, and on the composition of the thermite mixture. With a stoichiometric mixture preheated to a temperature of 570 K the temperature of the melt will be about 3270 K at the time of injection. This temperature can be lowered by reducing the initial temperature or by adding alumina or iron to the stoichiometric mixture.

It is evident from observations that the injected melt always contains a small portion of noncondensable gas that influences the melt mass flux in the nozzle at the end of the tube. This has also been shown by the AFDM calculations. In addition, part of the iron vapourizes following the pressure relief during the injection. Start and duration of the injection are controlled by two fast acting slide valves mounted in the connection tube between injector and sodium vessel. Both the tube and the nozzle have an internal diameter of 30 mm.

3. TEST PARAMETERS

The test parameters and some data of the four tests carried out are summarized in Table 1. The tests are listed in a chronological order.

Table 1: Significant Test Parameters, Initial Conditions and a few Experimental Data

Test No.		TH561	TH562	TH564	TH567
Main melt component		Al_2O_3	Al_2O_3	Iron	Iron
Melt temperature	K	2970	3270	3270	3270
Injection pressure	bar	25	25	25	25
Duration of injection	ms	170	153	136	123
Mass of melt injected	kg	5.5	4.1	5.5	4.9
Al_2O_3	kg	4	3.1	1.3	1.1
Fe	kg	1.5	1	4.2	3.8
Mean injection velocity	m/s	11.8	10	11.9	11.3
Sodium mass	kg	155	155	155	140
Sodium temperature	K	783-808	773-785	763-795	813-823
Sodium level	m	2.67	2.67	2.70	2.42
Cover gas pressure	bar	1.10	1.10	1.10	1.07
Vapour volume	m^3	0.081	0.079	0.089	0.084

The temperature of the melt cannot be measured during the tests; it has been derived from pretests. In the first test, TH561, the melt temperature was lowered by adding alumina to the thermite mixture. In the following tests, a stoichiometric thermite mixture was used. The molten mass injected is controlled primarily by the duration of injection and finally determined by a mass balance performed after the test. The smaller portions of iron in tests TH561 and TH562 and of alumina in tests TH564 and TH567 in the respective total masses reflect the incomplete separation of the melt components. Test TH567 was performed under the same initial conditions as TH564 in order to verify the reproducibility of experimental results.

The gas pressure of the injector system is set to a relatively high value (25 bar) in order to ensure that the driving pressure acting on the melt flow is always positive, i.e. the pressure difference between the pressure in the crucible and the average pressure in the thermal interaction zone,. The mean injection velocity (estimated from the melt mass and the time of injection) and the maximum vapour volume of the two-phase region are given in the table as an additional information. The latter was calculated from the maximum increase in the sodium level.

The initial sodium temperatures vary a little from test to test due to the heating procedure preceding the test. The cover gas pressure is kept constant in all experiments. The initial (static) pressure at the bottom of the sodium pool, p_o, is calculated to be approx. 1.3 bar. This pressure corresponds to a saturation temperature of 1180 K.

The choice of the two most significant test parameters, i.e. the temperatures of the coolant and the melt, respectively, ensures that, according to present knowledge, a vapour explosion does not occur. This item will be discussed in more detail further below.

4. EXPERIMENTAL RESULTS

4.1 General Remarks and Course of the Experiments

The general course of the experiments which throughout showed similar characteristics can shortly be described as follows:

Immediately after the start of injection, a two-phase region develops in the bottom part of the vessel caused by the thermal interaction of the melt and sodium. The growth and collapse of this zone are mainly determined by both the

balance of evaporation and condensation and the inertia of the sodium above the interaction region. During the injection period evaporation is dominant. The interaction region expands and, as a result of this, the sodium level increases. After the end of the melt injection condensation and gravity become dominant causing the upward movement of the sodium to slow down. Finally, the sodium flows down again and the two-phase region collapses. It is the period up to about the end of expansion that deserves our special interest. During this period, thermal energy is converted into mechanical energy.

In the following section, a detailed description is given of the two tests in which mainly iron was injected (TH564 and TH567). These tests are chosen because of their better instrumentation and improved data recording. They have been performed under almost identical initial conditions; therefore, they give also information about reproducibility. The results of the tests in which mainly alumina was injected (TH561 and TH562) are discussed afterwards. A comparison of the two types of tests, i.e. the discussion of the influence of the melt composition on the test results, is given in Section 8.

4.2 Tests Performed Mainly with Iron (TH567 and TH564)

To facilitate the comparison of the two tests with iron the most important data and results of the evaluation of both tests have been put together in one figure for each case. The sequences of events are discussed referring to Fig. 3, the development in axial and radial direction of the two-phase boundary is depicted in Fig. 4, and unfiltered pressure signals are plotted in Fig. 5.

In Fig. 3, the following characteristic data are drawn as function of time: (1) the pressures measured in the bottom part of the sodium pool and in the cover gas, (2) the upper boundary of the sodium, and (3) the axial extension of the two-phase region in which the interaction takes place. To enable the presentation of the sodium pressure on the given time scale, very short pressure peaks have been eliminated by filtering. The curves representing the rise of the sodium level were obtained by a special procedure using the measuring signals of the sodium level probe, of the temperature and void signals of the sensors in the upper part of the test vessel, and of the pressure signals. By this procedure no clear upper boundary of the sodium could be determined for the time after the maximum of the sodium level. Therefore, a shaded area marks the zone in which this boundary is supposed to be located. In case of the test TH567, the dashed line represents the signal derived from the level probe. The axial boundaries of the interaction region (two-

phase region) refer to a narrow zone close to the centre line of the test vessel where the maximum axial extension was measured.

Development of the two-phase region

The change of the sodium level as shown in Fig. 3 can be taken as a measure of the growth of the net vapour volume. Due to the inertia of the sodium above the interaction zone, the sodium level rises slowly initially. Compared to that, the extension of the upper boundary of the interaction region is much faster. This is shown qualitatively in Fig. 4 where the axial and radial development of the interaction region is depicted with the time as a parameter. The curves in this figure are derived from local measurements and show the maximum axial and radial extensions of the two-phase region while assuming rotational symmetry. The pictures show that, initially, the two-phase region grows axially and radially, the axial growth being larger by a factor of about five due to the direction of the melt jet. After the vapour has filled the whole cross section, the two-phase zone grows mainly axially. Of course, this behaviour is attributed to the relatively small vessel diameter.

On closer examination, a somewhat uneven development of the two-phase region, both spatially and temporally can be detected. In test TH564, the vapour front reaches the test vessel wall locally (at $z \simeq 350$ mm) after 60 to 70 ms, whereas full voiding of the cross section is reached much later, after about 160 ms, shown by the photo diode signals. In test TH567, complete voiding is reached a little earlier, namely after 140 ms. The unsymmetric development of the two-phase zone is supposed to be due to an unsymmetric front of the melt jet on entering the sodium pool. In fact, the form of the melt front is being determined by various factors, e.g. by the manner in which the melt flows through the connected pipe.

After the last thermal interaction, the two-phase region continues to expand axially due to the inertia of the liquid sodium above, certainly at a reduced rate. The maximum axial extension of the two-phase region is 1780 mm and 1920 mm in tests TH567 and TH564, respectively; this means that it remains below the throttle plate positioned at 2000 mm. It is only in test TH564 where a larger single bubble is registered above the throttle plate during the expansion phase. In test TH567, for example, the sodium level rises by about 1.27 m; this rise corresponds to a vapour volume of about 0.084 m^3 (cf. Table 1). The respective values of test TH564 are a little larger (0.089 m^3) which may be due to the larger melt mass

injected. Comparing these values one should keep in mind that the error band width is estimated to be about ± 3 - 5%.

It is deduced from the data base that the regions where thermal interactions mainly occur are the top of the two-phase region and the melt entrance region. This has been confirmed by calculations with AFDM [5]. The events that take place at the top of the two-phase zone are characterized by periods of intensive contacts between the front of the melt jet and sodium. These are dominated by sudden evaporation, pressure build-up and acceleration of the two-phase boundary, each followed by periods of reduced evaporation, pressure decrease, and deceleration of the two-phase boundary. In the bottom part of the test vessel, the liquid displaces much slower than at the top of the two-phase region. Underneath the lower two-phase boundary, liquid sodium tends to flow radially inward thereby contacting the melt jet. Subsequent evaporation pushes the liquid back and gives rise to an oscillating evaporation process.

The collapse of the two-phase region is indicated by the pressure peak at about 0.6 s. The exact location where the vapour finally collapsed cannot be determined from the instumentation; therefore, the boundary at the right-hand side of the interaction region is drawn by a dashed line in the diagrams of Figs. 3a and 3b.

Behaviour of the upper boundary of the sodium after the maximum expansion

At the time of vapour collapse the thermocouples in the former two-phase region show temperature increases of up to 250 K, related to the initial values, i.e., the sodium also in this region is still subcooled. Even if small regions existed of superheated sodium formed by the former boundary layer of the liquid phase which may give rise to a, probably limited, after-evaporation, the upper boundary of the sodium and, consequently, the pressure in the cover gas should return approximately to their initial values. The "new" value should show an increase which is due to the thermal expansion of the sodium, the increase in the gas temperature, and the volume of the melt injected. In fact, such an agreement is found in case of the cover gas pressure whose level is higher than the initial value by about 0.2 bar. This increase can be calculated taking into account the thermal expansion of the sodium estimated from the temperature measurements, the volume of the melt, and an increase of the cover gas temperature of 100 K.

In case of the sodium level, agreement is not found for the time of vapour collapse but several seconds later: After five seconds, for example, the sodium level shows an increase of about 60 mm which can be recalculated. This means that the behaviour of sodium level signal (cf. Figs. 3a and 3b) cannot be explained,

up to now, for the period of time from the beginning of sodium downflow till about 3-4 seconds after the vapour collapse.

Examination of the pressure signals

The signals of the pressure measured in the sodium are considered to be the most important ones because they give immediate and detailed information about the intensity of thermal interactions and help to identify different characteristic periods during a test. Moreover, combined with the change in the sodium level, the pressure signals are used to calculate the mechanical work. The signals of the pressure transducer P61 mounted near the bottom of the test vessel are presented in Figs. 3a and 3b. The general course is rather similar in both experiments. Several distinct pressure events can be observed during the time of injection. The steep pressure increase at the start of injection is caused by the first contact of the melt with the coolant which results in sudden evaporation.

It is about in the middle of injection when the value of the average pressure falls below the initial level for a short period of time; after that, it rises again. This behaviour may indicate that the formation of a two-phase region reduces temporarily the intensity of the thermal interactions and, consequently, the vapour production. Accordingly, the growth of the vapour volume is seen to stop for a short period of time expressed by the step in the sodium level curve, Fig. 3a, at $t=0.08$ s. There is also a feedback anticipated from the pressure build-up on the injection process. Because of the high imposed driving pressure on the melt this feedback is small, however.

The exponential pressure decrease starting about 10 to 30 ms after the end of injection, i.e. the time when the melt supply actually ends, indicates a sudden reduction of the intensity of the thermal interaction between melt and coolant. As a result of the reduced vapour production and because of the continuous increase of subcooled surfaces, condensation becomes dominant. Consequently, the upward movement of the sodium column above the reaction zone slows down and stops. Gravity forces and the pressure difference between the pressure in the cover gas volume and in the two-phase region become dominant and the sodium moves back again.

Evaluating the pressure signals one should keep in mind that the signals of the dynamic pressure transducers recorded during the period of thermal interaction always consist of a mixture of pressure waves originating from various sources including wave reflection. In this context it is interesting to know the pressure history inside the two-phase region and to compare it with the pressure recorded

in the liquid sodium nearby. Such a comparison is made in Fig. 6 where the thick dashed line represents the saturation pressure as a function of the temperature [6] measured at level $z = 400$ mm and at a distance of 100 mm from the vessel centre. The signal of the P62 pressure transducer located at $z=500$ mm is represented by the thin solid line. Additionally, the void signal V032 obtained from the same location as the temperature signal is drawn in the bottom part of the figure.

For $t < 0.040$ s the dashed line remains at zero level, i.e., the measuring point is still surrounded by subcooled liquid sodium; this condition is also indicated by the low level of the void signal. After that point in time, the temperature starts to rise due to the approaching two-phase boundary which passes the measuring point at $t = 0.045$ s. This event is indicated by the steep increase in the void signal. The first temperature peak reached at 0.059 s corresponds to a saturation pressure of 5 bar. After the relative minimum at 0.075 s, the saturation pressure is seen to follow, with a short time delay, the trace given by the average of the P62 pressure signal up to the maximum of about 9 bar at 0.14 s. Naturally, because of its lag time, the thermocouple is not able to reproduce high-frequency oscillations as shown by the pressure signal.

After the maximum, during the exponential decrease, the pressure measured in the sodium is constantly smaller than the saturation pressure. It can be concluded from this difference that there is a radial pressure gradient due to the flow of vapour which condenses at the circumference of the two-phase region. Later, towards the end of the decrease, both pressures fall even below the initial level.

Details of the pressure history can be better discussed using the unfiltered signals. For this, the signals of the pressure transducer P61 covering the period of thermal interaction have been chosen (cf. Fig. 5). The pressure events are seen to consist of a sequence of low-frequency variations of the average pressure superimposed by high-frequency pressure peaks. This is true for both tests and, additionally, one can state that the time histories of both tests show a rather similar frequency spectrum.

The first "pressure event" starts at zero time; it is characterized by a steep increase and lasts about eight milliseconds. The pressure peaks superimposed amount up to 30 bar. They are caused by a sequence of local evaporation and condensation processes. This assumption is in agreement with the information derived from the time histories of both the void signals and the void fraction data discussed in the preceding paragraph. The frequency of the pressure peaks

reduces from 1600 Hz in the beginning to about 500 Hz in the middle of the injection period; the frequency increases again toward the end of and after the injection period.

Reproducibility

Summarizing the discussion above with regard to corresponding results which were found in pressure time history, growth of the two-phase region and maximum vapour volume, a high degree of reproducibility can be stated for the two tests with iron.

4.3 Tests Performed Mainly with Alumina (TH562 and TH561)

Results of the tests with alumina are given in Fig. 7 where pressures, the upper boundary of the sodium, and the axial growth of the two-phase region are shown. The spatial and temporal development of the voided region is plotted in Fig. 8; the unfiltered sodium pressure signals are shown in Fig. 9.

As can be seen from these figures, the sequences of events are similar to those encountered in the tests with iron. Therefore, only special features and deviations to previous results are discussed in this section. Comparing the results of the two tests, one has to take into account (1) the restricted instrumentation available in test TH561, (2) that the melt temperature in test TH561 was lower by 300 K and (3) the injection time was longer which yielded a larger melt mass injected (+34%). Items (2) and (3) resulted in a thermal energy disposable which is about 15% larger than in test TH562 (cf. Table 3).

Development of the two-phase region

The start of the sodium level rise in test TH562 (Fig. 7) is delayed by a few milliseconds compared to that in test TH561, whereas the rate of the rise is larger than in test TH561. It is assumed that the delay has something to do with the amount of non-condensable gas contained in the melt that is probably markedly larger in test TH561 than in the three other tests. The presence of non-condensable gas which is known to reduce the heat transfer between the melt and sodium may be responsible for a reduced vapour production immediately after the start of injection and, hence, for the delayed rise of the sodium level.

The growth in axial direction of the interaction region is about the same in both tests with alumina during the first 30 ms. After that, this rate is faster in case of TH562. This behaviour can also be deduced from Fig. 8. It can be seen in this figure that in test TH561, the diplacement of the sodium in the bottom region of

the test vessel occurs in a more incoherent manner than in test TH562. In this context it is interesting to compare the times at which the upper boundary of the interaction region, respectively two-phase region, arrives at certain axial levels. These data are compiled in Table 2. One can see that, despite of the different initial rates of growth, the level of 1.5 m is reached in the three relevant tests (TH562 - TH567) at the same time, 200 ms. Similarly, it is at about the same time, that the maximum axial extension of the two-phase region was obtained in the three tests. These extensions were found to be 1780 mm in tests TH562 and TH567 and 1920 mm in test TH564.

Table 2: Data Showing the Axial Growth of Two-Phase Region

Test No.	Time in ms needed to reach the axial level of			Max.extension mm
	1000 mm	1500 mm	maximum	
TH561	120	1)		
TH562	80	200	310	1780
TH564	130	200	320	1920
TH567	130	200	320	1780

1) there is no instrumentation above 1000 mm

The maximum axial extension of the two-phase region could not be evaluated for test TH561 because of the restricted instrumentation. For the same reason no statement can be given wether or not or at which time the cross section of the test vessel had been fully voided.

Regarding the maximum vapour volumes obtained in the tests with alumina one can state that they are nearly identical (about 0.08 m^3., cf. Table 1) and are reached at the same time (0.31 seconds, see Fig. 7). In the tests with iron, the maximum vapour volumes are larger by about 6 - 10%. This result is due above all to the larger impulse $\int p\,(t)\,dt$ of the second pressure rise taking place towards the end of injection (cf. signals P61 in Figs. 3 and 7).

In test TH562, the vapour collapses at time 0.645 s which is 40 - 60 ms later than in the tests with iron whose collapse times are close together. The collapse time in test TH561 is relatively late, 85 ms later than in test TH562. Condensation pressure peaks in the tests with alumina show the lowest amplitudes, about 3 bar each, whereas 4 bar and 12 bar were measured in the tests with iron.

Examination of the pressure signal

The start of test TH562 is characterized by two single, relatively low pressure peaks (cf. Fig. 9). After a short delay of 4 ms, a series of much higher pressure peaks (up to 58 bar) whose minima remain at a rather low level for a couple of milliseconds indicate the start of intensive thermal interaction. Since the melt detector in test TH562 responds one millisecond prior to the series of high pressure peaks, it is assumed that it was the presence of non-condensable gas that attenuated and/or delayed by a few milliseconds the first effective contact between the melt and the sodium.

In the following time, the characteristics of the pressure signal in test TH562 are quite similar to those in the tests with iron. The frequency of the pressure peaks decreases from 1600 Hz at the start of the high amplitudes to about 460 Hz in the middle of the injection period. Here, the amplitudes reach values of up to 18 bar. The decline of the pressure in the sodium after injection is similar in both tests but somewhat slower than in the tests with iron. From this one can deduce that, after the injection, the intensity of thermal interaction decays at a lower pace in case of alumina, influenced by the different physical properties, such as heat capacity, thermal conductivity, heat of fusion, etc...

5. RELEASE OF MECHANICAL ENERGY

As shown, sodium vaporization during thermal interaction leads to the expulsion of the sodium above the zone of interaction. This means that sodium vapour is the dominant working substance for the conversion of thermal into mechanical energy. The conversion ratio is used as a measure for the violence of thermal interaction processes.

The mechanical work was calculated using the equation

$$E_{mech} = \int_{t=0}^{t_e} p_1\,(t)\,dV \qquad (1)$$

where

$p_1(t)$	is the time history of the pressure signal P61 (z = 100 mm)
$dV = A\,dz_l$	is the change in the two-phase volume,
t_e	is the time when the vapour volume is maximum,
A	is the vessel cross-section,
$z_l = f(t)$	is the time history of change of the sodium level

The potential of thermal energy, E_{therm}, of the melt is calculated assuming cooling down of the melt from the initial value to 1180 K, i.e. the saturation temperature of the coolant at 1.3 bar.

The energies thus obtained, the conversion ratios, E_{mech}/E_{therm}, and the ratios of max. vapour volume to thermal energy are summarized in Table 3. Obviously, both ratios are higher in the cases when mainly iron was injected. This may be an indication of a higher effective heat transfer coefficient. Nevertheless, the conversion ratios are generally low, thus confirming the test result insofar as an energetic large-scale vapour explosion did not occur.

Table 3: Energy Conversion Data

Test No.	E_{therm} MJ	E_{mech} MJ	E_{mech}/E_{therm} %	V_V/E_{therm} dm^3/MJ
TH561 (Al_2O_3)	15	0.019	0.13	5.4
TH562 (Al_2O_3)	13	0.022	0.17	6.1
TH564 (Fe)	12.5	0.026	0.21	7.1
TH567 (Fe)	11	0.033	0.30	7.6

More information can be obtained from the characteristics of the time dependent increase of the mechanical energy. The curves depicted in Fig. 10 have been calculated using Eq. (1). Roughly speaking, the increase in mechanical energy occurs in a form represented by a double "S" curve. This means that a short-term accelerated initial increase and a long-term steep increase toward the end of injection time are separated by a short period of a reduced increase ($t \approx 60 \ldots 90$ ms). The latter period corresponds to the period in which the characteristics of the sodium pressure signal undergo changes; here, the lowest frequency of pressure peaks and a short-term fall below the initial value of the minima of the pressure are observed (cf. Fig. 5).

The last inflection point of the curves is noted about 20 ms after the end of injection as indicated on the abscissa. As mentioned above, this is approximately the point in time when the tail end of the melt enters the interaction region; after that time, the intensity of thermal interaction is reduced resulting in a decrease of vapour production.

6. ASPECTS OF A VAPOUR EXPLOSION

In this section the conditions will be examined for a vapour explosion to occur in the THINA tests. This is done on the basis of Fauske's contact temperature hypothesis [7]. Accordingly, explosions may occur if the instantaneous interface temperature, T_I, arising upon first contact, is higher than the spontaneous nucleation temperature T_{SN} of the coolant.

The conditions prevailing in the THINA tests are discussed using Fig. 11 where the abscissa and the ordinate represent the temperatures of the hot component (melt) and of the cold component (sodium), respectively. The operation points determined by the THINA test conditions are entered as dots. The threshold lines for the above criterion, marked $T_I = T_{SN}$, are obtained under the condition that the interface temperature is equal to the spontaneous nucleation temperature of sodium (=2060 K) as derived by Zimmer [8]. The contact temperature was calculated using formulas given in [9].

Another criterion to be considered is the minimum film boiling temperature T_{min} that must be exceeded by the coolant temperature to establish the necessary condition for stable film boiling. The latter ensures low heat transfer rates from the melt particles to the surrounding coolant during the so-called premixing phase. On the basis of experimental findings Zimmer et al. [10] derived the following relation for T_{min}:

$$T_{min} = 1600\ K + 7.2\ (T_{sat} - T_C), \qquad (2)$$

where T_{sat} and T_C are the coolant saturation temperature and the actual coolant temperature, respectively; T is expressed in K.

On the basis of Fig. 11, one finds that the condition for T_{min} is not fulfilled due to the large coolant sub-cooling. On the other hand, Fauske's condition, $T_I > T_{SN}$, is fulfilled for iron but not for alumina. Still no large-scale vapour explosion has occurred in the tests with iron. This finding can possibly be explained by the absence of premixing without much heat transfer that is considered to be also a precondition for a vapour explosion. The reason why this condition is not met might be the absence of sufficiently stable film boiling. However, some sort of film boiling must occur because, as stated before, the contact temperature for iron is higher than the homogeneous nucleation temperature. From the characteristics of the pressure signals shown in Figs. 5 and 9, one can conclude

that thermal interaction takes place exclusively as a sequence of small local events.

Summarizing these considerations, one can presume that incoherent boiling phenomena dominate at first contact. These are, indeed, not sufficient to produce premixing of large amounts of the melt.

7. POST-TEST EXAMINATION AND FRAGMENTATION OF THE MELT

The post-test examinations show that melt fragments were deposited on the lances up to 1.4 m height in test TH564 and up to 1.2 m in test TH562. This means that the melt penetration depths are markedly smaller than the maximum axial extensions of the two-phase region.

Most of the debris of the melt were deposited at the bottom of the vessel and a smaller portion was swept out into the filter of the sodium supply system. After separation from the remaining sodium by vacuum distillation the sizes of the fragments were analysed. The particle size distributions of the four experiments are shown in Fig. 12. About 90% of weight of the fragments are less than 1 mm in diameter and about 40 to 50% less than 0.25 mm.

The debris are generally a mixture of spherical particles and rugged fragments. Differences are found in the appearance and shape of the fragments. In the tests where alumina was the dominant melt component the particles of alumina larger than 0.25 mm are generally rugged with smaller iron particles embedded. In the tests with iron most of the debris show a mossy structure; it must be added that pure globule forms are more frequent than in the tests with alumina.

8. DISCUSSION OF THE INFLUENCE OF THE MELT COMPOSITION ON THERMAL INTERACTION

One of the objectives of the experiments was to find out the influence of different physical properties of the two main melt components, alumina and iron, on the course of thermal interactions as well as on the potential of a vapour explosion to occur. Besides, the reproducibility of the tests was also to be examined. As already stated, good reproducibility was obtained in case of iron. A comparison between the two tests with alumina is restricted since both the melt temperatures and the melt masses injected differ considerably.

In spite of the difference existing in the physical properties of the main melt components, the general course of events was similar in all tests. Some minor

differences are found in the pressure histories, especially in the early phase. The most striking characteristics, i.e. differences, will be outlined in the following.

In the initial phase of the tests which is characterized by an immediate pressure rise with high-frequency pressure peaks, the amplitude of the peaks are highest in one of the tests with alumina. It is in this test where a short delay in the pressure rise is stated which is supposed to be due to a larger portion of gas contained in the melt. Later, in the middle of the injection period, the pressure peaks are higher in case of iron than in case of alumina.

Differences are found in the amounts of the maximum axial extension of the interaction region and in the higher energy conversion ratio. Both are higher in case of iron. This result is due above all to the higher impulse of the second pressure rise, $\int p(t)\,dt$, towards the end of injection. The maximum extension of the two-phase region was reached in all tests at the same time though the initial rise of the upper boundary was faster in case of alumina. The pressure decline after injection is slower and the rise of the collapse pressure pulse is lower in the case of alumina.

Though in the case of iron the instantaneous interface temperature was higher than the spontaneous nucleation temperature of the coolant, in each case the test conditions were too far away from the threshold of the minimum film boiling temperature. Above all, the low sodium temperature is supposed to be responsible for the fact that only incoherent boiling phenomena dominate at first contact.

From the above statements, with one exception, no immediate conclusion can be drawn with regard to a marked influence on the thermal interaction of the different physical properties of the materials. This exception is the appearance that the effective heat transfer coefficient was a little larger in case of iron since the yield of vapour related to E_{therm} was slightly larger (cf. Table 3). In judging these effects, one should keep in mind that the melt injected was always composed of three quarters of one component and one quarter of the other.

9. SUMMARY AND CONCLUSIONS

The behaviour of fuel-coolant interactions which might occur during whole-core disruptive accidents of LMFBRs is being investigated out-of-pile in the THINA test facility. The molten core materials are simulated by a thermite melt. In each test about 5 kg of melt consisting of either mainly alumina or mainly iron were injected within 130-170 ms into a pool containing 150 kg of sodium. It is

concluded that a small amount of non-condensable gas was present in the melt jet in all cases. The experimental data which have to be assessed with regard to the test conditions and the geometry applied are well suited for validation of computer codes. The results can be summarized as follows:

- The general course of events was simular in all experiments , i.e., a marked influence of the different physical properties of the two main components, iron and alumina, on the interaction process cannot be stated yet.

- Thermal interactions occurred mainly during the injection period. In all experiments phases are observed of alternating intensities of the vaporization and condensation processes.

- Because of a pronounced sub-cooling of the coolant large-scale vapour explosions did not occur. The interaction is considered to occur as a sequence of small local pressure events.

- The melt penetrated up to 1.4 m into the sodium pool. The maximum axial extension of the coherent interaction region was quite larger, 1.8 - 1.9 m; thereby, it remained below the throttle plate.

- Maximum void fractions of about 100%, related to the cross section of the test vessel, were observed locally and temporarily.

- The conversion ratios from thermal to mechanical energy were generally low, about 0.13 - 0.17% in the case of alumina and up to 0.30% in the case of iron.

- The particle size distribution of the melt fragments was similar in all tests. Differences were observed in the shape and the appearance of the particles of the respective melt components.

10. REFERENCES

[1] W. MASCHEK, A Brief Review of Transition Phase Technology, KfK 3330, Karlsruhe (1982).

[2] WILHELM and W.R. BOHL, "The AFDM Models for Interfacial Areas and Their Test on Out-of-Pile Experiments," Proc. Int. Fast Reactor Safety Meeting, Vol. IV 437, Snowbird, USA, August 12-16, 1990

[3] F. HUBER, K. MATTES, W. PEPPLER, Experiments with Injection of Thermite Melt into Sodium, Proc. NURETH-4 Conference, Vol. 1, 290, Karlsruhe, Oct. 10-13, 1989.

[4] F. HUBER, A. KAISER, W. PEPPLER, Experiments on the Behaviour of Thermite Melt Injected into a Sodium Pool, Proc. Int. Fast Reactor Safety Meeting, Vol. II, 407, Snowbird, USA, August 12-16, 1990.

[5] D. WILHELM, F. Huber, A. Kaiser, Numerical Simulation of the THINA Thermite Injection into Sodium with the AFDM-Code, ANP Conference, Tokyo (Japan), October 1992.

[6] A. PEE, Stoffdaten von Natrium, KFK 924, Karlsruhe (1969).

[7] H.K. FAUSKE, On the Mechanism of Uranium Dioxide-Sodium Explosive Interactions, Nucl. Sc. Eng., 51, 95, (1973).

[8] H.J. ZIMMER, Investigation of Vapor Explosions with Alumina Droplets in Sodium, KfK 4574, Karlsruhe (1991).

[9] H.S. CARSLAW, J.C. JAEGER, Conduction of Heat in Solids, §11.2 IV, Oxford University Press, London (1959).

[10] H.J. ZIMMER, W. PEPPLER, and H. JACOBS, Thermal Fragmentation of Molten Alumina in Sodium, Proc. NURETH-4 Conference, Vol. 1, 268, Karlsruhe, Oct. 10-13, 1989.

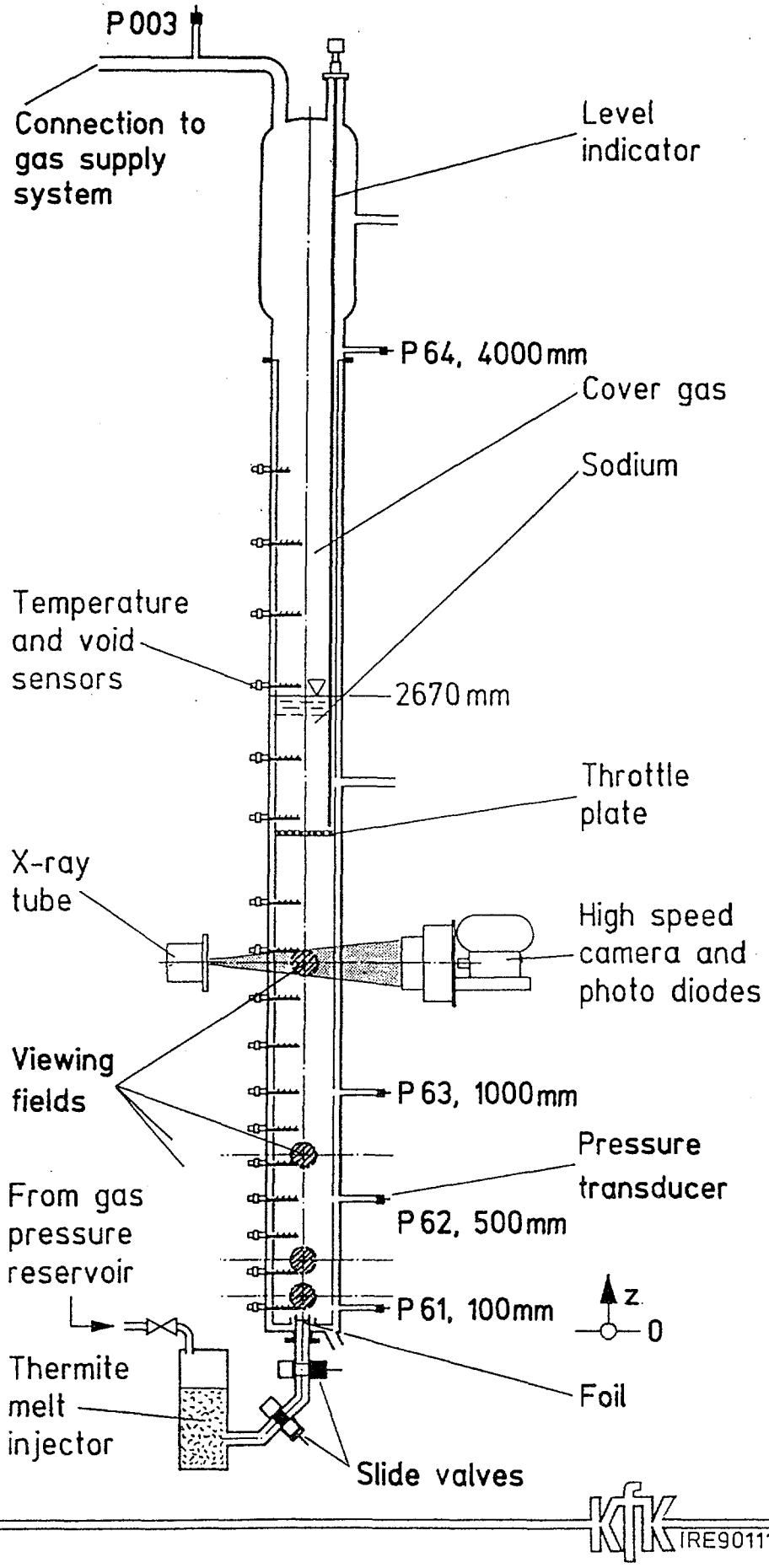

Fig. 1 THINA Test Vessel with Instrumentation (diameter 0.3m, height 5m)

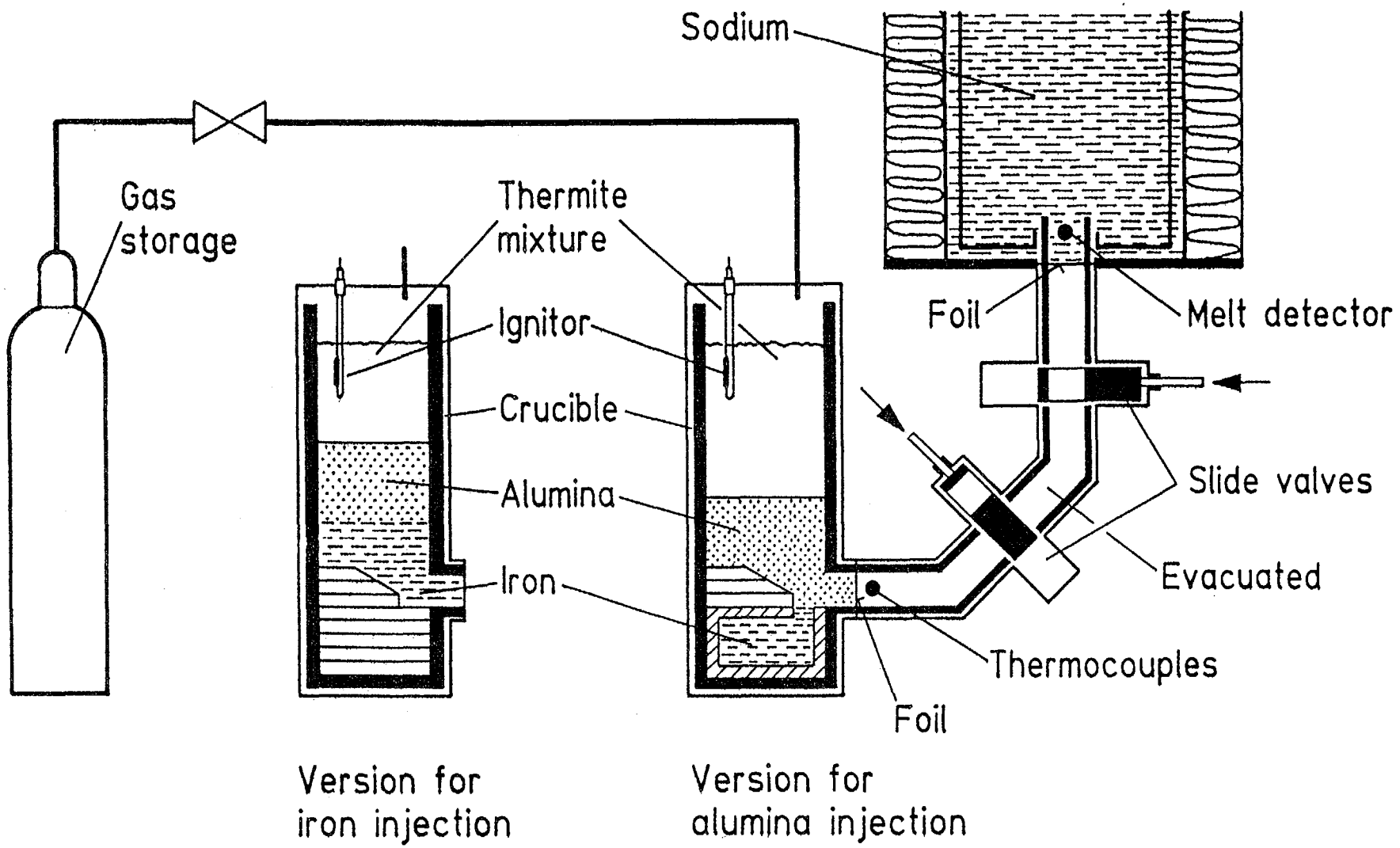

KfK IRE 89101759

Fig. 2 THINA Compact Injector (Version for Single-Phase Melt Injection)

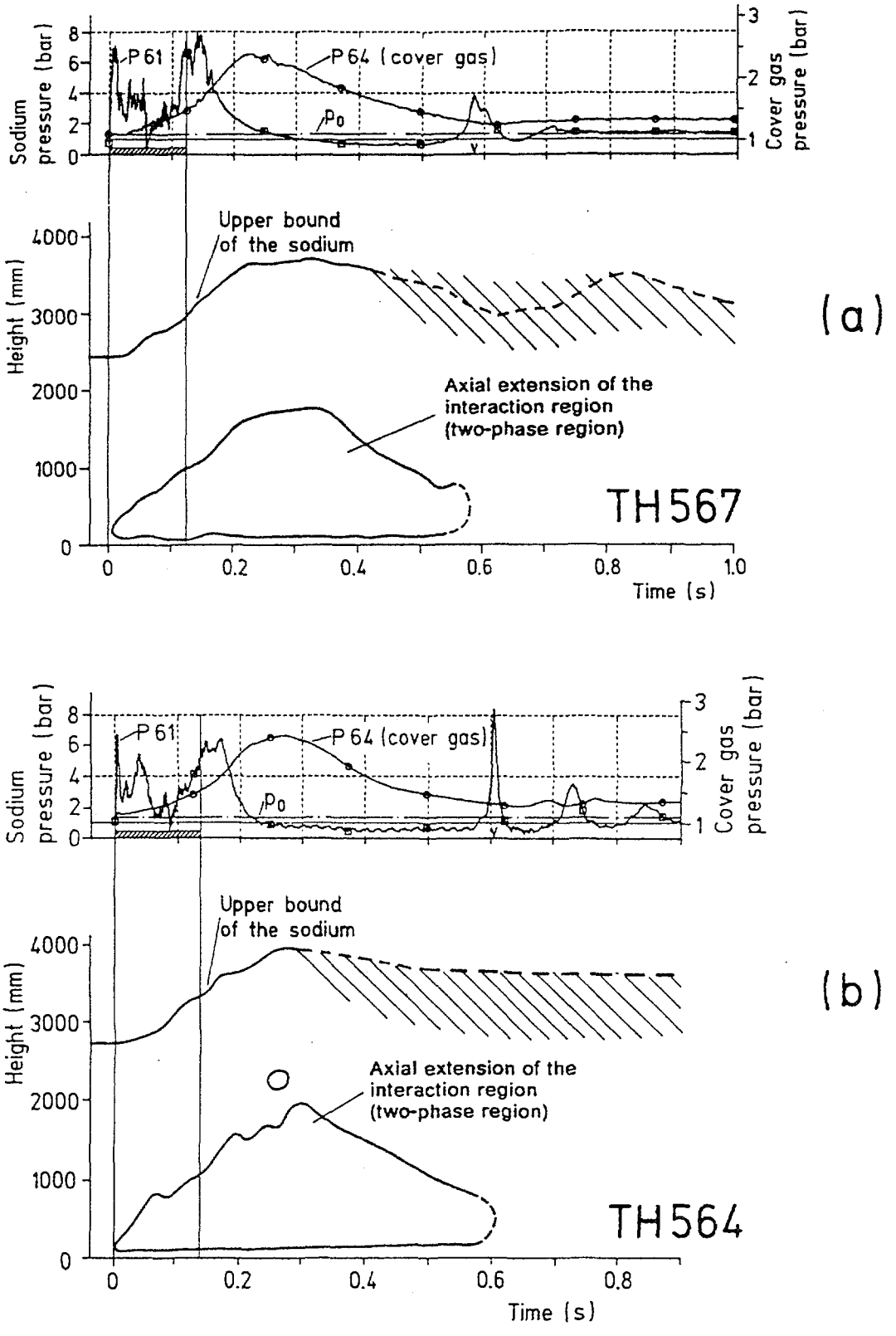

Fig. 3 Characteristic Data of the Tests with Iron Showing the Sequence of Events: Pressure Signals, Upper Bound of the Sodium, and Axial Development of the Interaction Region near the Vessel Centre. p_o is the Initial Pressure at z = 100 mm.

IRS9341909

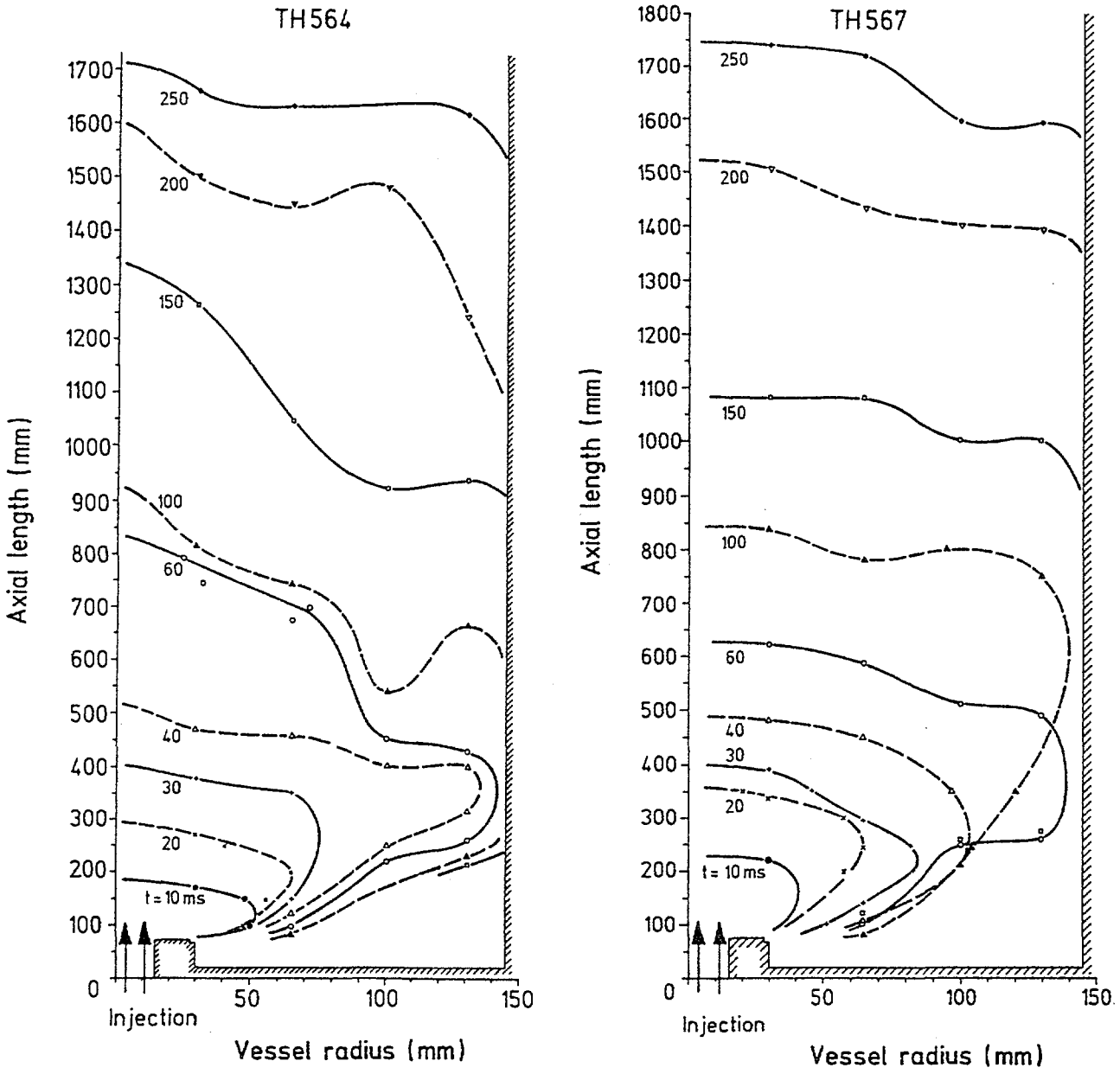

Fig. 4 Axial and Radial Development of the Two-Phase Region in the Tests Performed with Iron. The Time is Taken as a Parameter.

IRS9341910

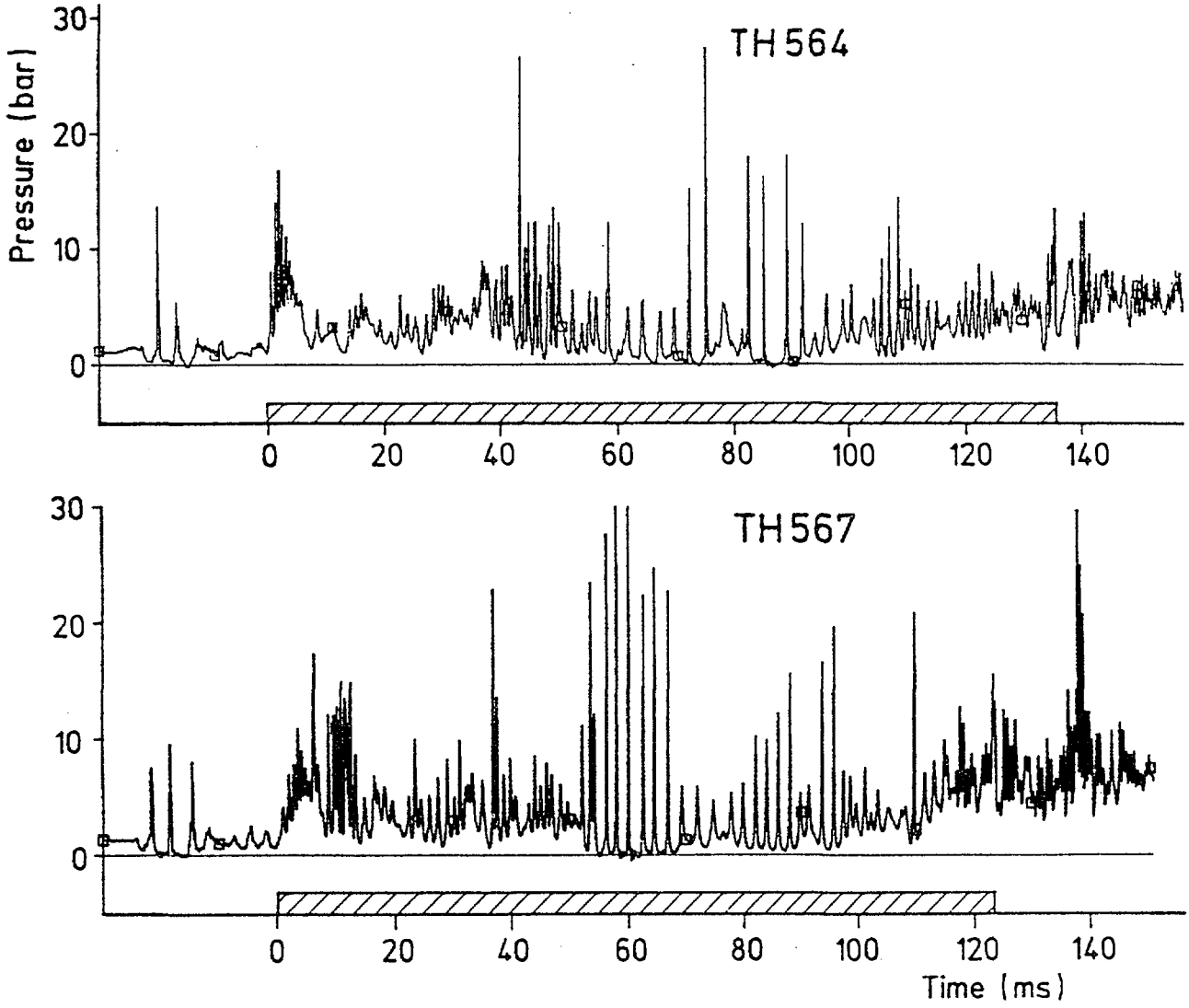

Fig. 5 Time Histories of the Sodium Pressure (z = 100 mm) of the Tests with Iron in a Better Time Resolution. Sampling Frequencies: 16 and 7.5 kHz in TH567 and TH564, respectively.

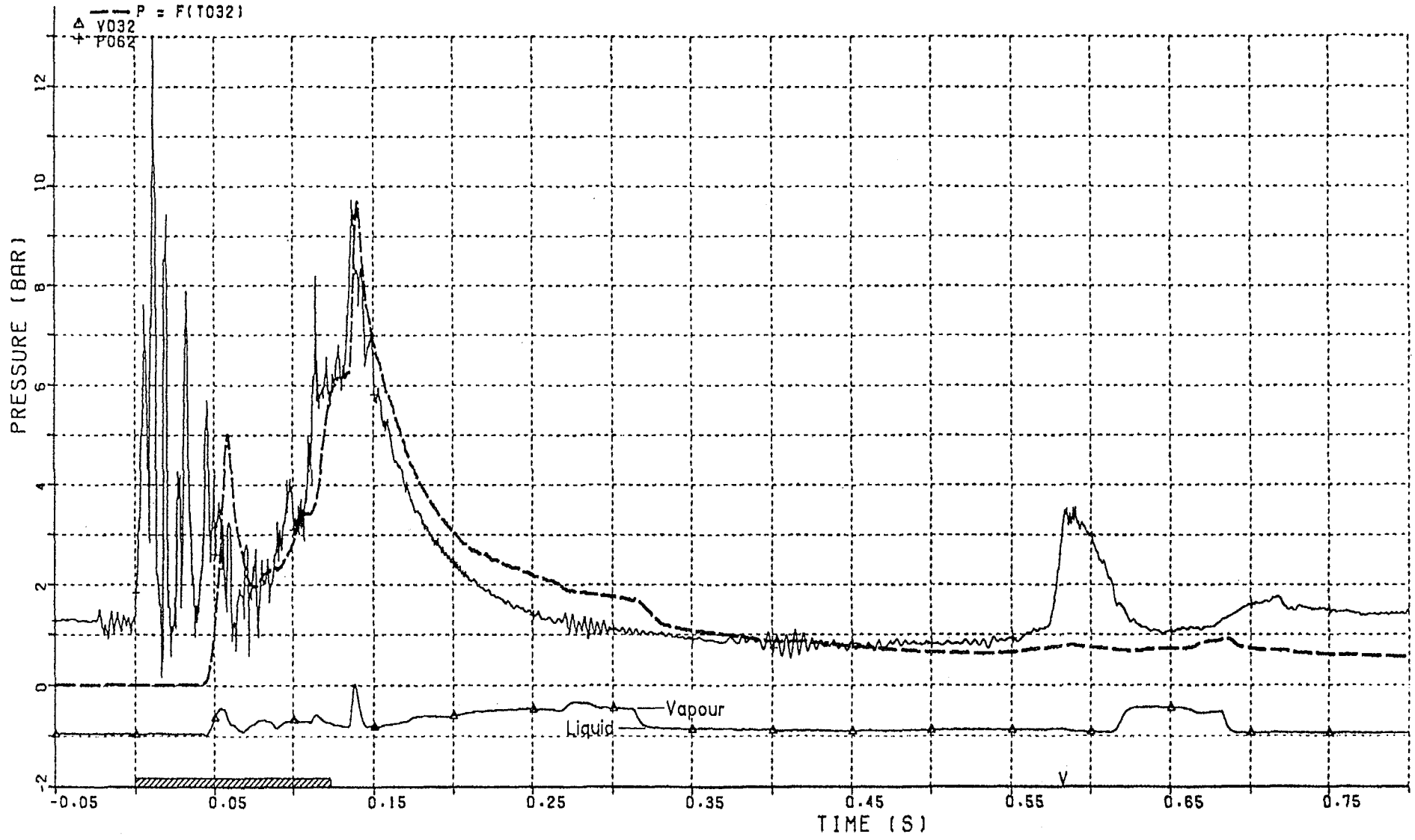

Fig. 6 Test TH567: Saturation Pressure as a Function of Temperature Signal T032 (z = 400 mm) Compared with Signal of Dynamic Pressure Transducer P062 (z = 500 mm). The Void Signal Shows Locally the Phases of Liquid and Vapour

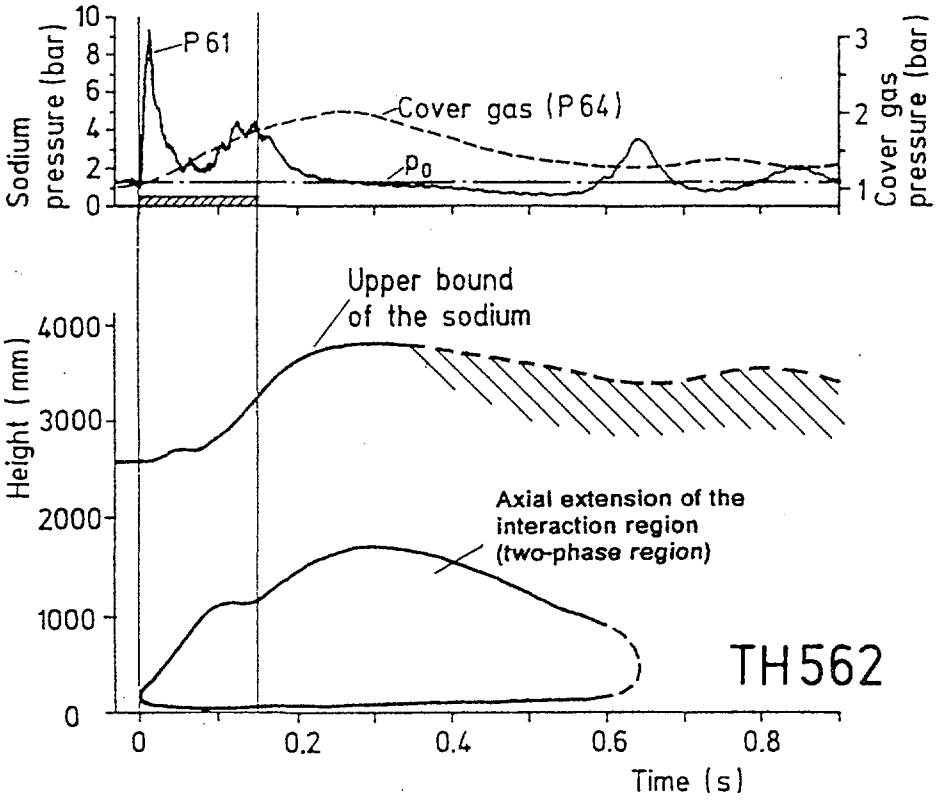

(a)

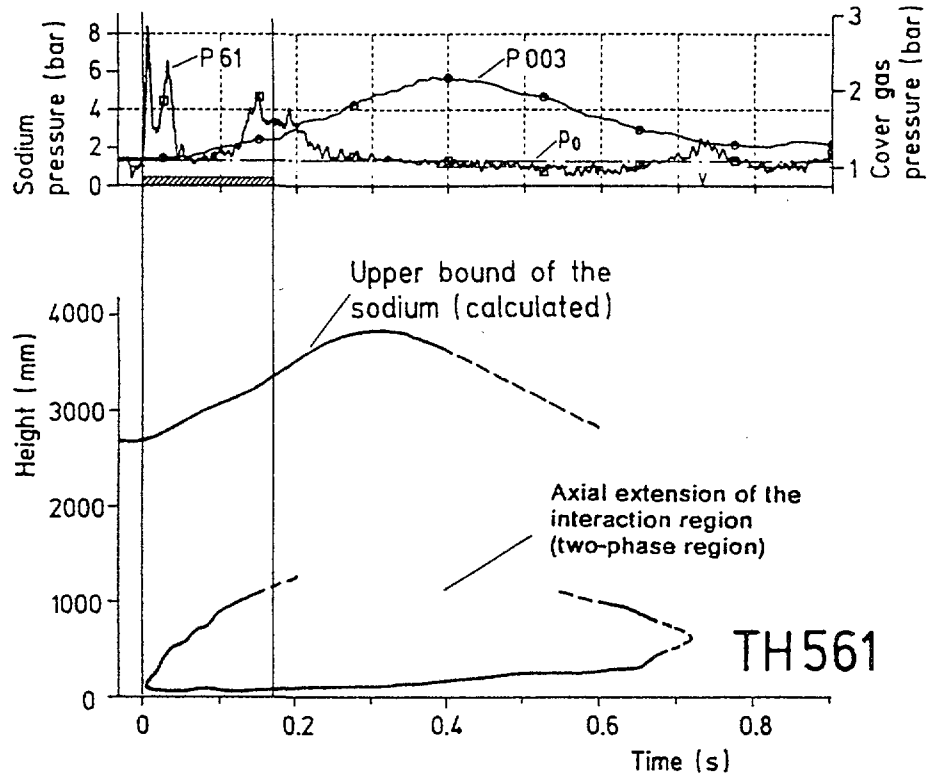

(b)

Fig. 7 Characteristic Data of the Tests with Alumina Showing the Sequence of Events: Pressure Signals, Upper Bound of the Sodium, and Axial Development of the Interaction Region near the Vessel Centre. p_o is the Initial Pressure at z = 100 mm.

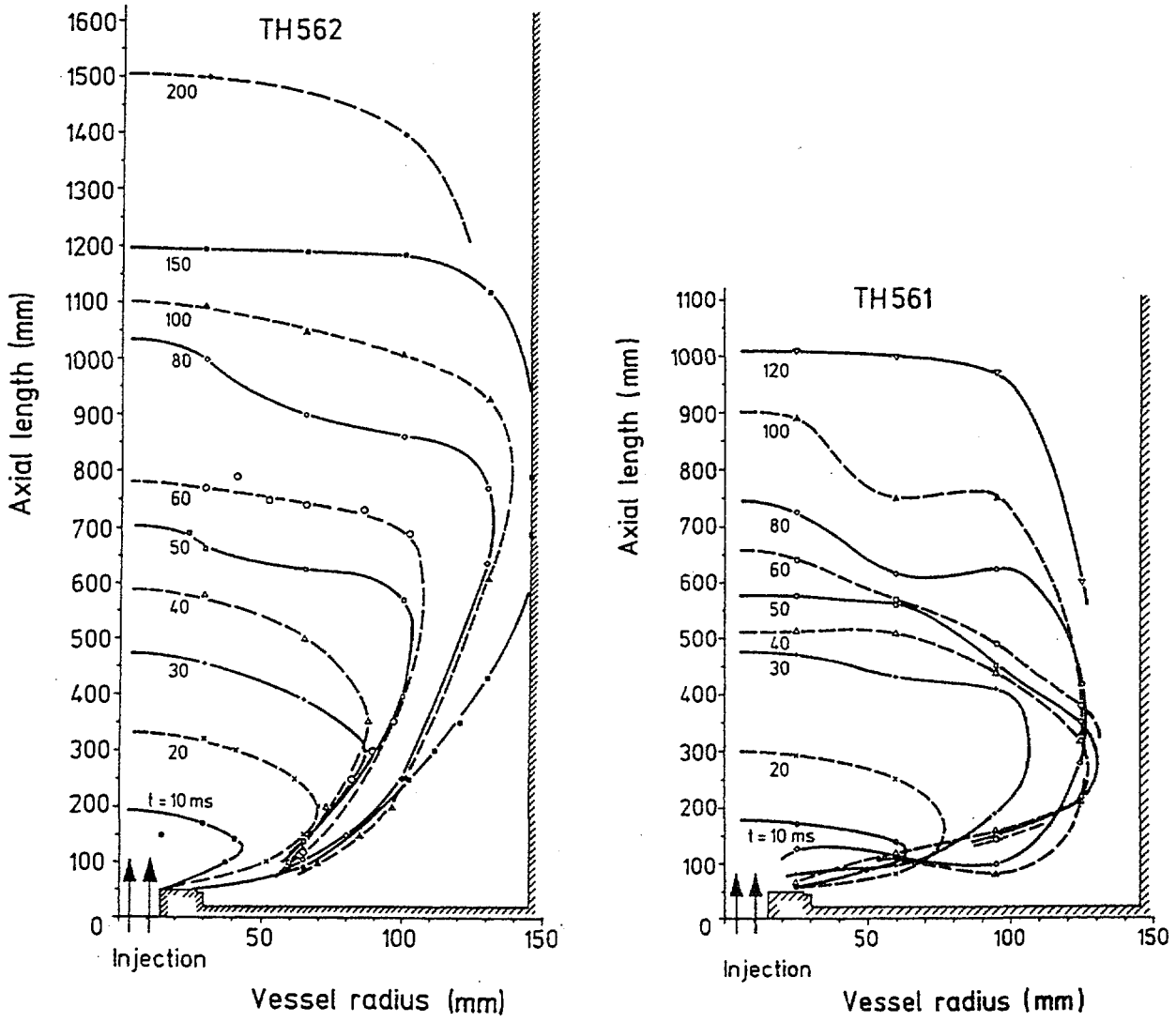

Fig. 8 Axial and Radial Development of the Two-Phase Region in the Tests Performed with Alumina. The Time is Taken as a Parameter.

IRS9341913

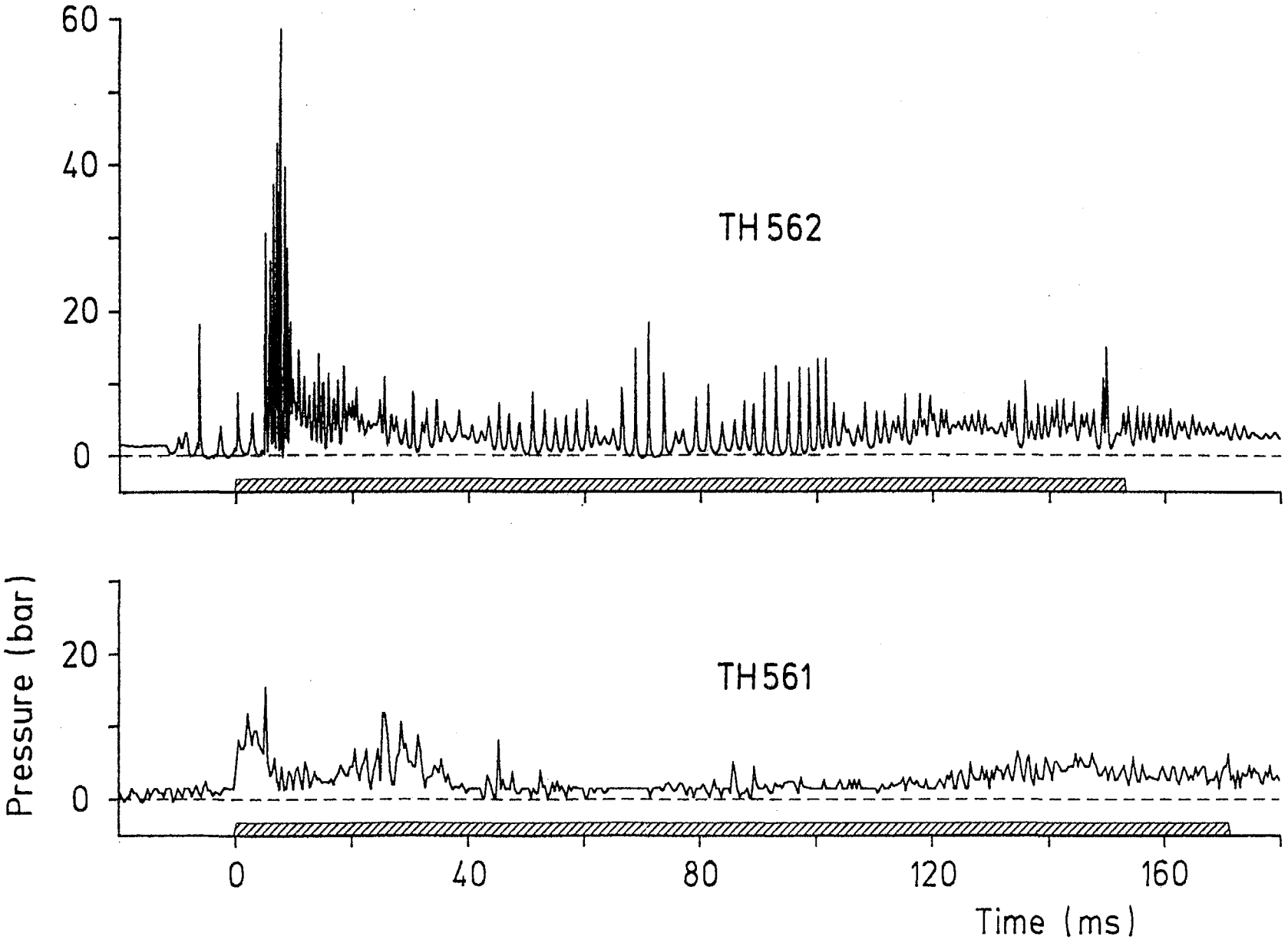

Fig. 9 Time Histories of the Sodium Pressure (z = 100 mm) of the Tests with Alumina in a Better Time Resolution. Sampling Frequencies: 5 and 1.25 kHz for TH562 and TH561, respectively.

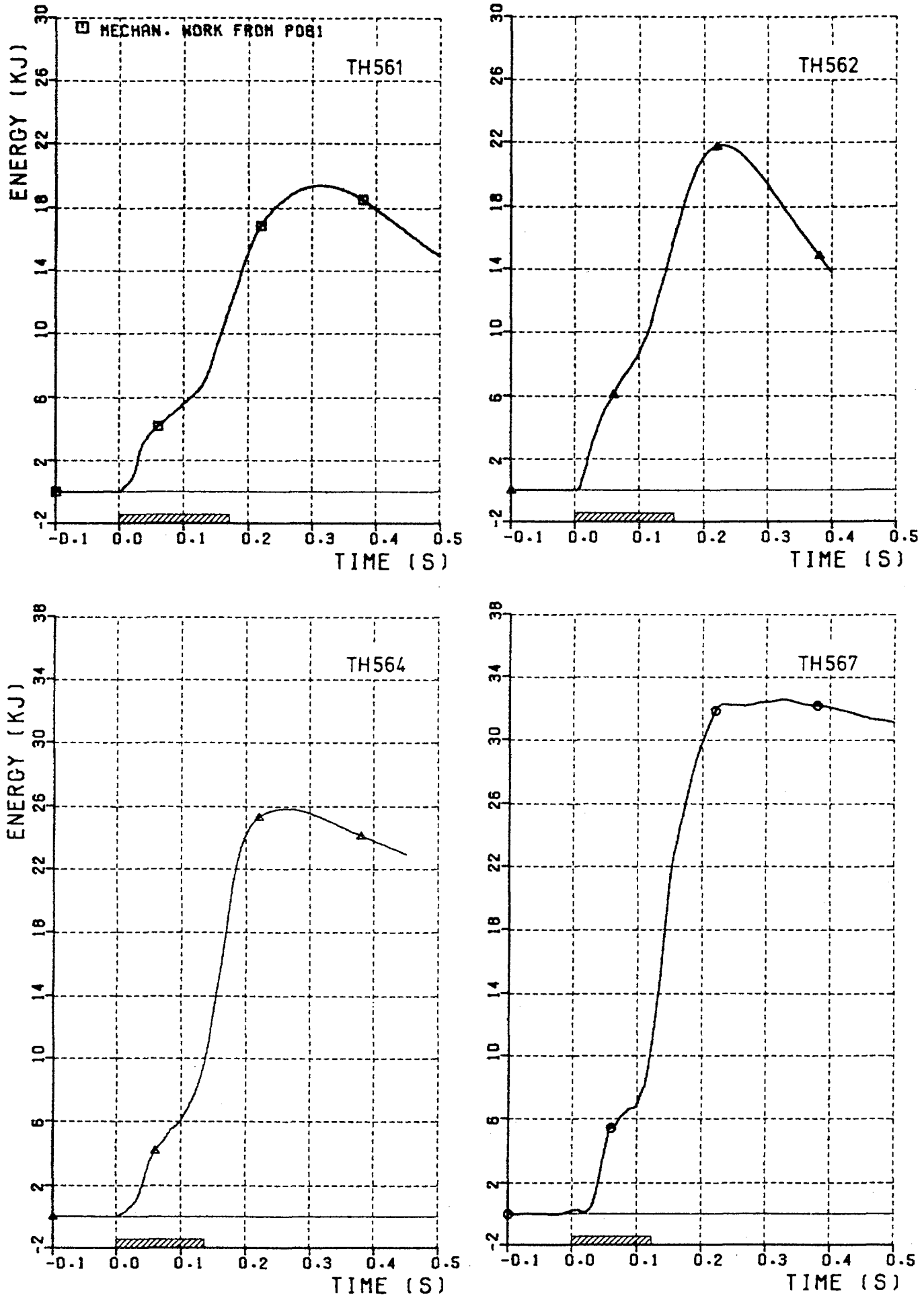

Fig.10 Histories of Mechanical Energy Formation (Eq. 3)

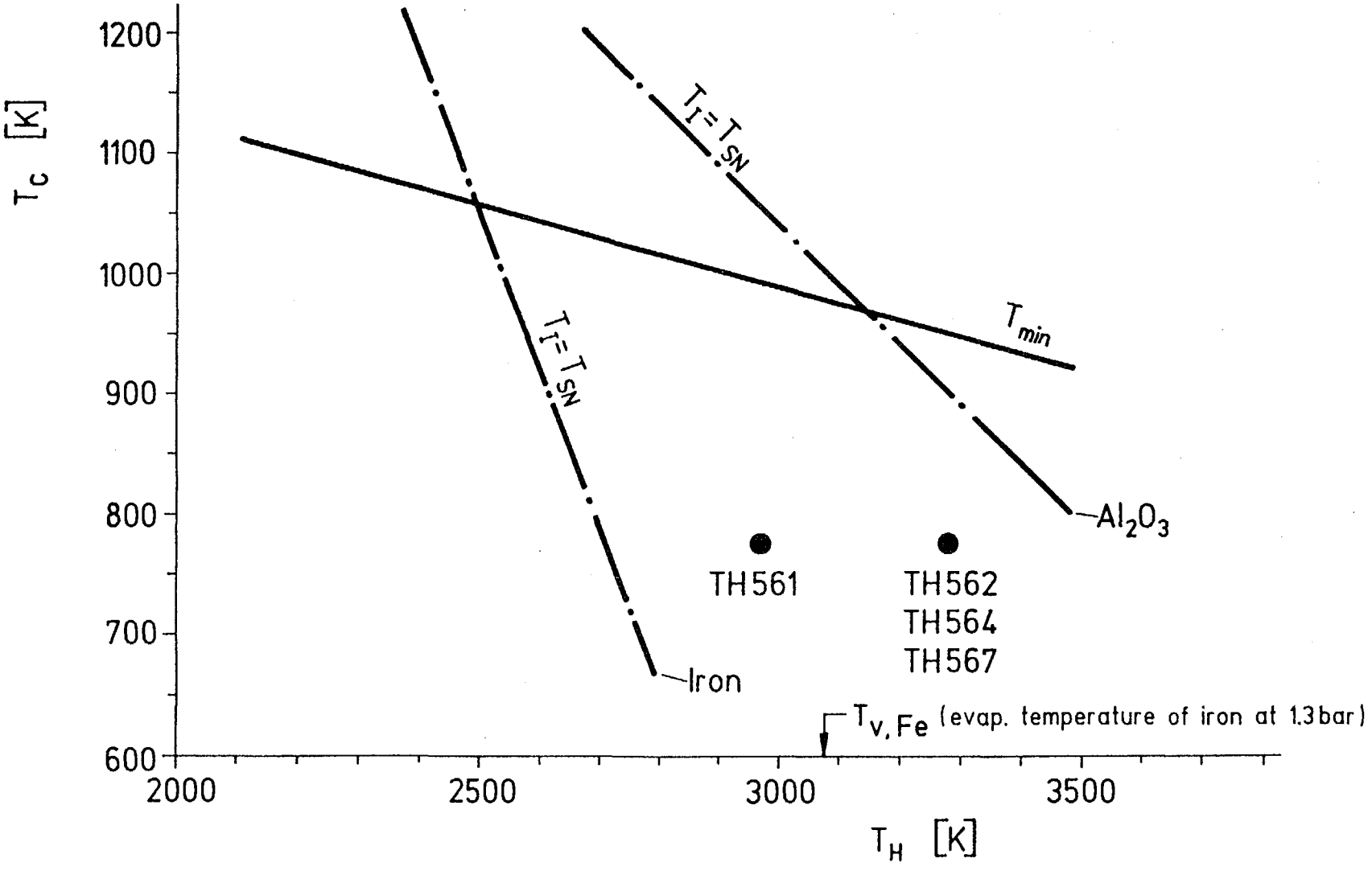

Fig. 11 Temperature Thresholds for Film Boiling (T_{min}) and for Spontaneous Nucleate Boiling (T_{SN}) for the Thermite Melt / Sodium System. • = Operation Point

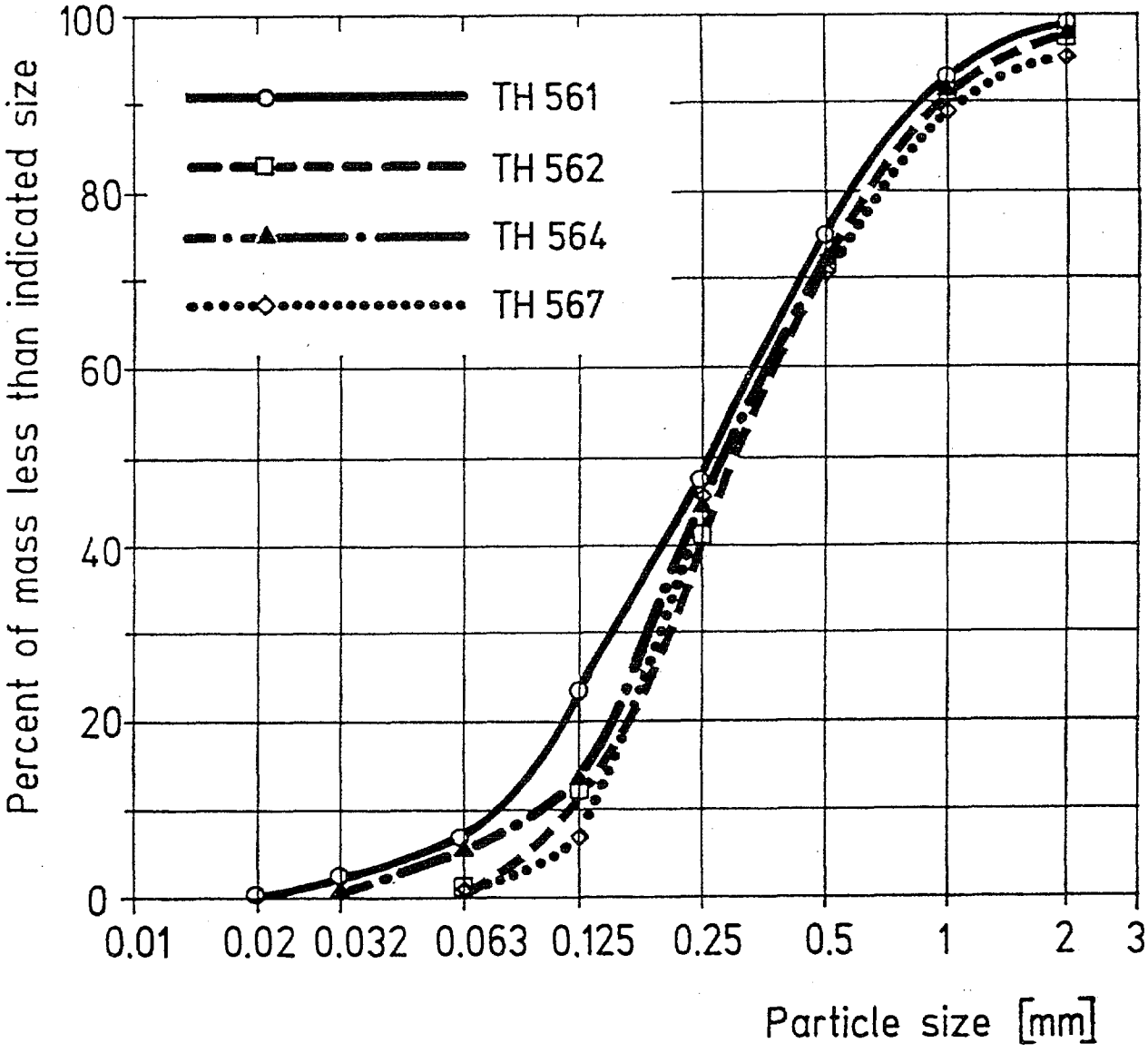

KfK IRS 926 2298

Fig.12 Particle Size Distribution of the Melt Fragments